Journal of Intelligent Systems and Internet of Things
Vol. 18, No. 01, PP. 238-249, 2026
DOI: https://doi.org/10.54216/JISIoT.180118

Cloud IoT with Remote Sensing Data Segmentation and Classification Using Deep Learning Model for Sustainable Agriculture

T. Shanmugapriya[1,*], RM. Rani[2], Gaddam Ravindra Babu[3], T. Srinivasulu[4], S. Saranya[5], S. Gopinath[6], M. Rajesh[7]

[1]Assistant Professor, Department of Computer Science and Business Systems, KPR Institute of Engineering and Technology, Coimbatore, India

[2]Assistant Professor, Department of Information Technology, SRMIST, Ramapuram, Chennai, India

[3]Assistant Professor, Department of Computer Science and Engineering, Koneru Lakshmaiah Education Foundation, Bowrampet, Hyderabad, Telangana, India

[4]Assistant Professor, Department of Information Technology, Aditya University, surampalem, Andhra Pradesh, 533437, India

[5]Assistant Professor, Department of Artificial Intelligence and Data Science, St Joseph's Institute of Technology, Chennai, India

[6]Assistant Professor, Gnanamani College of Technology, Namakkal, Tamilnadu, India

[7]Department of Computer Science and Engineering, Aarupadai Veedu Institute of Technology, Vinayaka Mission's Research Foundation (DU), Tamilnadu, India

Emails: priyamoons@gmail.com; ranir@srmist.edu.in; ravindragaddam@gmail.com; tsrinu531@gmail.com; ssaranrahul@gmail.com; sgopicse@gmail.com; rajesmano@gmail.com

Abstract

Sustainable Development Goals of United Nations are focused on enhancing agricultural production that has the potential to be transformational at the local as well as the global level. The available technologies in agriculture management that are based on Internet of Things (IoT) encourage sustainable production of more food by farmers, which contributes significantly to the achievement of these SDGs. The aim of this research is to propose novel technique in sustainable agriculture field analysis based on cloud IoT model with remote sensing and deep learning model. Here the cloud IoT model is used in agriculture field based remote sensing data analysis. This image has been segmented using watershed K-means temporal neural network (WKMTNN) and classification is carried out using deep quantile regressive Boltzmann machine (DQRBM). The experimental analysis has been carried out in terms of random accuracy, average precision, sensitivity, specificity for various agriculture field dataset. Proposed model attained average precision 96%, sensitivity 93%, random accuracy 98%, and Specificity 95%. These results highlight the superiority of the moisture estimation framework against their regression-based counterparts.

Received: February 28, 2025 Revised: June 01, 2025 Accepted: July 10, 2025

Keywords: Sustainable agriculture; Field analysis; Cloud IoT model; Remote sensing; Deep learning model

1. Introduction

Sustainable agriculture measures the sustainability and durability of food grains produced in an environmentally friendly manner. Sustainable agriculture encourages farming practices and approaches that support farmers and resources. Apart from its economic feasibility, it also maintains soil quality, reduces soil degradation, conserves water, increases land biodiversity, and ensures a natural and healthy environment. Reducing greenhouse gas emissions, stopping the loss of biodiversity, and protecting natural resources are all made possible by sustainable agriculture. Sustainable agriculture makes it feasible to raise agricultural output while protecting the environment and meeting the fundamental needs of coming generations. The core accomplishments of smart farming in terms of sustainable agriculture—which leads to a safer environment overall—include crop rotation, managing nutritional deficits in crops, managing pests and diseases, recycling, and water harvesting [1]. Biodiversity is essential to all living things, however things like garbage emissions, fertiliser and pesticide use contaminate it, decaying dead plants, etc. Humanity will have to face significant obstacles to sustainability in the twenty-first century. Agricultural systems will face pressure from the need to boost agricultural output in order to guarantee food security for a world population that is predicted to reach 9–10 billion people in next decades and from a changing climate that jeopardizes sustainability. UN Secretary-General recently issued a warning to the world community, stating that sea level rise, more extreme weather will affect humanity, and that climate change is happening faster than society is addressing it. These claims are corroborated by recent publications issued by United Nations Intergovernmental Panel on Climate Change [2]. The likelihood of erosion in agricultural systems will rise as extreme weather events occur more frequently. Since conservation, techniques are essential for preserving and boosting agricultural systems' sustainability and productivity, humanity will not be able to adjust to a changing climate without them. To meet nutritional requires of a future human population of 9–10 billion, food production is estimated to need to expand by 60–100% by 2050. Food security for billions of people was made possible by the Green Revolution, which included these technologies [3, 4]. The challenges of the twenty-first century, however, are different. To ensure food security, soil and water conservation will be crucial, and sustainable precision agriculture and environment (SPAE) is required to prevent further effects from intensive agriculture and climate change that could hasten the pace of climate change. It is impossible to overlook constraints including operational complexity, high initial cost, enormous data requirements, and information accuracy [5]. The authors [6] employ blockchain to mitigate security breaches, facilitating the creation of a decentralized distributed blockchain method that is also transferred across IoT cluster chiefs. Therefore, in order to guarantee safety of agricultural output and rigorously adhere to the food safety red line, it is imperative that majority of nations in world actively support coordinated development of PA, remote sensing (RS), machine learning (ML). Without explicit programming, ML is a technique for data analysis that enables computer methods to automatically discover patterns and rules in data. For feature collection as well as categorization, prediction, or decision support, researchers typically employ machine learning (ML) as an integrated framework. As the processing power of big data has increased, many traditional methods are refined and optimized; new models and methods are constantly being developed [7].

2. Literature review

Research has focused on the application of ML, DL, and IoT systems, specifically for precision farming. The relevance of crop production forecasting for traders, agri-businesses, as well as governmental institutions was demonstrated in [8]. Their research, however, progressed into the question on whether machine-learning models could be used instead. In particular, they assessed how well various machine-learning models predicted yields of cluster beans in the Bikaner district of Rajasthan. Interestingly, the most effective model using Support Vector Regression with a linear kernel, had the highest R2 (98.31%) values which validates its usefulness for predicting agricultural yields regardless of the location and adequate data. To avoid the following damage by pests, the author [9] incorporated DL for Disease and Pest Detection. Work [10] introduced an IoT device that had some ML capabilities. It integrates several soil sensors and algorithms that help in monitoring the soil and providing recommendations for different types of crops. This particular gadget can be attributed use of advanced technology in the agricultural sector as it was able to improve food production and management of the available resources. Smart irrigation systems where installed by the author [11] to enhance irrigation efficiency and to conserve water in water deficient regions. Work [12] presents a solution to challenges faced in agriculture in India using IoT and DL technologies. It uses the automation of field monitoring and weather forecasting to increase productivity of crops and facilitate disease prediction. The forecast technology enables farmers to raise their productivity as it provides 94% accuracy in weather forecasting and provides 98% in field monitoring techniques. In this regard, the author [13] stresses the weight of livestock management relative to the agriculture sector by suggesting a multi-layered approach that integrates DL and IoT technology for effective monitoring in real time. In this case, the system detects challenges related to animal welfare through the DL analysis, enriches with sensors to gather information and processes the information to eliminate all the outliers. The

considerations for the future research lines are given based on the experimental outcomes which are aimed at producing increases in a cost beneficial way. Work [14] presented a methodology that employed ML and IoT in harvesting and post-harvest management, which reduced food waste, and also makes supply chain works better. A unique idea and framework for lip reading using RF sensing with WiFi and radar technology is discussed in [15]. By Lip reading, they recognize the speech from the movement of lips and mouth under facemask. They use VGG16 architecture, which is a deep convolutional neural network (CNN). It has 16 layers and is trained in large-scale image recognition. Their work is also noninvasive and can work in noisy environments along with covered faces. Another diverse application is discussed in [16]. They use RF sensors and WiFi to study the distinction between risky and safe driving practices. They utilized recurrent neural networks (RNNs) to process time series data. The networks managed long-term dependencies and get around the issue of vanishing gradients. The models are bidirectional long short-term memory (BI-LSTM) as well as gated recurrent unit (GRU). Their technique can notice minute variations in the driver's vital signs and body language. Author [17] focuses on determination of a person's sleeping posture. The authors use frequency-modulated continuous wave (FMCW) radar for the said purpose. The technique divides the radar pictures into four postures. The postures are supine, prone, left lateral, and right lateral. They use a CNN classifier. The technique is non-invasive and effective in busy, dark areas.

3. Proposed cloud IoT model in remote sensing imaging

For static objects, post-cloud solutions can help reduce latency and jitter, but they do not work for moving objects that are aware of their surroundings. As more and more data are created at the edges of the networks, the speed of data transit grows and becomes an issue for cloud centered computing. When the data is processed and stored in the cloud, there is no guarantee that data kept confidential, that there would be any feedback, or the feedback will be given in real time. Both latency and jitter must be improved due to the large number of devices. Furthermore, since the devices are always in motion and power is never sufficient, cloud communication is always problematic. The concept has been to shift the processing and storage of information closer to the end users who create such data in order to lessen the bandwidth usage and cloud congestion. Such includes organizing the information and decoding it. To cope with these challenges, a host of fundamental models have been put forward, which ity integrated cloud computing to edge of network. Each of these systems oversees the movement of containers or Virtual Machines (VMs) between physical servers, if necessary, changes the way services are delivered based on the end users' locations. In addition, these three approaches allow the creation of federated systems, which are built from several edge systems that can share resources and communicate. There are many regions where agricultural sustainability has been reported to work. In "smart agriculture," use of DL has gone mainstream, leading to sophisticated as well as pleasant manufacturing results.

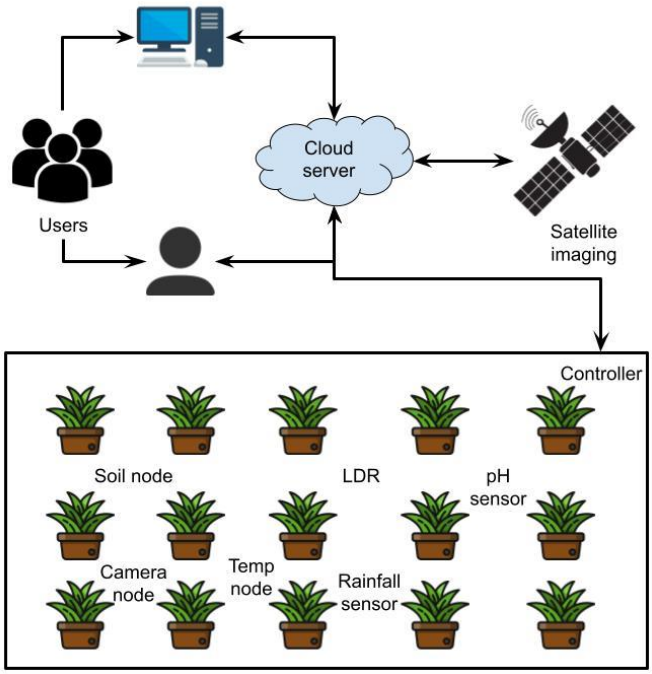

Figure 1. Flowchart of remote sensing and satellites images techniques in smart farming.

The ultimate aim of data coziness in any data storage is analysis preparation. Thus, it implies homogeneity. In case of simple and small scale remote sensing analysis; there is no much concern on the extent of homogeneity within the raster data layers as mostly the computation is carried out within a scene by a single processing node. Hence, we suggest a data model that is more efficiently in data organization in regards to the data structure and data production techniques owing to the increasing need for better organization of remote sensing data due to the increasing spatiotemporal scales. For example, in cloud computing large-scale analysis aimed at certain application scenarios (algorithms, parallel computing strategies, etc) it should be clear that a remote sensing data model needs to be used. Acquisition of drone aerial imagery and high-resolution satellite images, especially for smallholder farms that are financially constrained, is very expensive. Also understanding the concept of a certain image requires experts in data processing and remote sensing. There is need to train the farmers on how to read the pictures and even involve people who can assist in reading the images and extracting meaningful information. In order to address this challenge, the technology should be improved, the costs of data collection and analysis should be reduced, and farms should be equipped and trained. In addition, integrating these satellite and remote sensing images with other information sources helps to enrich the knowledge of some few attributes. Fig. 1 below describes flow chart of smart farming employing satellite sensor and remote sensing approaches.

4. Watershed K-means temporal neural network in segmentation

The watershed transform consists in flooding the image regions and finding the height of the water surfaces where waters from different regions meet. This method has successfully addressed numerous image segmentation problems that involve processing of complex shapes. As an image segmentation technique, the watershed algorithm has been most popular due to the first implementation in computer vision based on mathematical morphology. It is easier to describe this idea in a program. In the given instance, we will explain how such implementation might look like. Every image being worked on, is treated as a three dimensional surface. Following this logic, every area with lesser height is assumed to be filled with water source. Thus, readings of the picture pixel densities are considered as encumbrances on surface elevation. In a valley, water level increases continually until it is about to flow into rejoining sections, and walls are provided in between them to prevent the flow. The element clusters of the segmentation and the catchment basins formed by the watershed of the topographic surface in the images under consideration correspond to one another. K-implies bunching is a common system. The k-implies bunching calculation group's information by iteratively figuring a mean strength for each class and sectioning the picture by ordering every pixel in the class with the nearest mean. The calculation includes an extreme partner work as its bunching idea; where the information is grouped into the extended region allow us to take a picture, Y with M information to be grouped into N territory. From the start, all center qualities are discretionarily assigned. The jth data, wj is allocated to the closest data cluster, Dk based on the least Euclidean distance [8], where j = 1,2,3,4, … , … M. and K = 1,2,3,4, … , … , N. Subsequent to completing the allocating cycle for all information, the new area of focuses is assessed by eqn (1):

$$D_k = \frac{1}{p_k \sum_{j \in D_k} W_j} \qquad (1)$$

Where, pk is number of partners in kth group. The strength of each cluster is then determined in the calculation utilizing by eqn (2)

$$g(D_k) = \sum_{j \in D_k} \left(\| W_j - D_k \| \right)^2 \qquad (2)$$

After arranging the mid values in a sorted order there are two values are recorded to retrieve the clustering process, those are the mid least strong point Dq and mid high strong point Dt . In order to obtain the best clustering process the following condition must be satisfied by the link between Dq andDt by eqn (3)

$$g(D_q) \geq \propto_b g(D_t) \qquad (3)$$

In the above condition the constant value ∝b=∝0 where ∝0 is with the distinctive value 0 < ∝0 < 1 3 . The mid least strong point Dq withdrew all its associates when the above condition is not satisfied. When the above condition is accepted then it obtains the Dt associates which contains least strong point i.e. Wj < Dt . For the associates of Dt with more value than Dt they will remain as Dt associates. Both Dq and Dt will be updated using above conditions by eqn (4)

$$D_Q = \frac{1}{p} \sum_{J \in D_Q} W_J$$

$$D_t = \frac{1}{p_t}\sum_{j\in D_t} W_j \quad (4)$$

The introduction of companions Dq and Dt into the equation also bears newcomers PQ and Pt. Given that the Eucledian metrics from the center worth to its counterparts is small, it can be observed that a cluster whose information value is closer to the center value tends to take assimilate the least strong value (for instan ce the case could be true for Dq). Thus, when the center Dq is compelled to downsizing, the tendency is that a significant portion of the data set gets discarded. In this case, group dynamics can also shift. Therefore, it can be illustrated weak segmentation is quite apparent. Subsequent to completing the moving technique, all middles are rearranged utilizing and the new area, everything being equal, the estimation of ∝b is then redesigned by eqn (5)

$$\alpha_b = \alpha_b - \frac{\alpha_b}{N} \quad (5)$$

All above-expressed strategies are rehashed until it is fulfilled. To guarantee an improved bunching measure, another state as characterized by estimation is locked in. The total methodology will be rehashed if estimation is not fulfilled by eqn (6)

$$g(D_q) \geq \alpha_c g(D_t) \quad (6)$$

Specifically, certain notions can be put into proper use in practice with the implementation of space and time. For instance, we can develop deep learning models that integrate the basic principles of temporal deep learning models together with those of graph representation learning. Such spatiotemporal deep learning models have a temporal DL block to incorporate the new temporal knowledge, and a graph NN block that performs message-passing in a given time point when the model operates on a sequence of temporal graphs. It allows for the sharing of relevant spatio-temporal regional influences between different spatial units in the model. By taking use of fused methods end-to-end differentiability, the temporal and spatial layers that are combined into a single parametric ML method are trained collaboratively. Predicting spatiotemporal data produced b y a network of sensors is one common problem that calls for cross-node federated learning constraint. In this case, V represents the collection of sensors, while E denotes the relationships between the sensors.

As input to the GN, central server gathers concealed state from every node $\{\boldsymbol{hc}, \mid i \in \mathrm{V}\}$. Each GN layer in the manner described below eqn (7) updates input features

$$\mathbf{e}'_k = \phi^e\left(\mathbf{e}_k, \mathbf{v}_{r_k}, \mathbf{v_{sik}}, \mathbf{u}\right) \vec{\mathbf{c}}'_i = \rho^{\epsilon\to 0}(E'_i)\,,$$

$$\mathbf{v}'_i = \phi^v(\bar{c}'_i, \mathbf{v}_i, \mathbf{u})\ \bar{c}' = \rho^{e\to u}(E')\,,$$

$$\mathbf{u}' = \phi^u(\bar{\mathbf{e}}', \bar{\mathbf{v}}', \mathbf{u})\ \bar{\mathbf{v}}' = \rho^{z\to u}(V') \quad (7)$$

3) in which e, v, and u stand for edge, node, and global features, respectively. These neural networks are called ϕ, ϕv, and ϕu. The aggregation functions $\rho\ e\!\!\rightarrow$, $\rho e\!\!\rightarrow\!\!u$, and $\rho v\!\!\rightarrow\!\!u$ include summation. For every experiment, we select a 2-layer GN with residual connections, as seen in Figure 1b. Assigning empty vector to u as input of first GN layer, we set vi = $\boldsymbol{hc}$, ek = Wrk,. For every node, server-side GN generates embeddings $\{\boldsymbol{hG},, \mid i \in \mathrm{V}\}$ and transmits corresponding embedding for every node.

5. Deep quantile regressive Boltzmann machine based classification

Let us assume that there is an available panel data on wages for a number of women (N) over a period of time (T) for the researcher. The aim of this research is to assess the relationship between income (y) and motherhood, as determined by number of children (x), while controlling for other variables including marital status, education, occupation, \ work experience (z). The panel data can separate the unobserved individual time-invariant characteristic (di) from the unobserved error term (uit), which is a by-product of sx;z that is positive definite and an i.i.d. random variable (vit). If sx;z is fixed, then the variance of uit is said to be homoskedastic, otherwise it varies with respect to x or z which represents a heteroskedastic error by eqn (8)

$$y_{it} = b_0 + b_x x_{it} + b_z z_{it} + \delta_i + u_{it}$$

$$u_{it} = v_{it} \times \sigma_u(x_{it}, z_{it})$$

$$v_{it} \sim \text{ iid } (0,1) \quad (8)$$

Assume that for every individual i, unobserved effect di is a parameter that must be evaluated in equation (9), the set of parameters $\beta = [b_0, b_x, b_z]$ and $\Gamma = \left[\hat{\delta}_1, \ldots, \delta_N\right]$ that best fit the data

$$\hat{\beta}_{obs}\hat{\Gamma}_{obx} = \min_{\hat{\beta},\hat{\Gamma}} \sum_{i=1}^{N} \sum_{r=1}^{T} \left(y_{it} - \hat{b}_0 - \hat{b}_x x_{it} - \hat{b}_z z_{it} - \hat{\delta}_i D_i\right)^2 \quad (9)$$

The number of data points is represented by word i. The quantile regression model equation for the th quantile can be expressed as follows, which is a comparable structure to the linear regression model by eqn (10)

$$Q_\tau(z_i) = \alpha_0(\tau) + \alpha_1(\tau) y_{i1} + \cdots + \alpha_p(\tau) y_p \; i = 1, \ldots, n \quad (10)$$

As a result, alpha coefficients are now quantile-dependent functions. Lastly, Eq.(11) can be used to illustrate the panel quantile regression model.

$$Q_r \mathrm{z_{in}} \left(\tau \mid \mathrm{z}_{i,-1}, \mathrm{x_{it}}\right) = \mathrm{c_i} + \gamma(\tau)\mathrm{z}_{\mathrm{i},-1} + \mathrm{x^T}_{\mathrm{it}}\beta(\tau), \mathrm{i} = 1, \ldots, n. t = 1, \ldots \mathrm{T_i} \quad (11)$$

where xit represents the exogenous variables, ς=(ς1,…,ςN)′ indicates N×1 vector of intercepts, zit is the predicted output, and zit−1 is the lag of the zit. The quantile, τ, of interest is permitted to influence the covariates' (zit−1,xit) effects (12):

$$Q_{Y_{it}}(\tau \mid y_{it-1}, \mathbf{x}_{it}, \boldsymbol{\theta}_i(\tau), \boldsymbol{f}_t) = \alpha_i(\tau) + \lambda_i(\tau) y_{it-1} + \mathbf{x}'_{it}\boldsymbol{\beta}_i(\tau) + \mathbf{f}'_t\gamma_i(\tau), \quad (12)$$

$$\mathbf{x}_{it} = \boldsymbol{\mu}_i + \Gamma'_i \mathbf{f}_t + \boldsymbol{v}_{it} \quad (13)$$

We begin by going over the case without taking into account any previous knowledge. Maximization of likelihood function, or, conversely, log-likelihood, is thus found to be identical to maximization of posterior distribution by eqn (14)

$$\mathcal{L}(\{\boldsymbol{s}^\mu\} \mid \mathbf{J}, \mathbf{h}) = \frac{1}{M}\sum_\mu \left[\sum_{i=1}^{L} h_i\left(s_i^\mu\right) + \sum_{i<j} J_{ij}\left(s_i^\mu, s_j^\mu\right)\right] - \log Z(\mathbf{J}, \mathbf{h}) \quad (14)$$

A straightforward gradient ascent technique can theoretically find the ideal set of parameters because it is simple to demonstrate that log-likelihood is a globally convex function of unknown values. More specifically, the following update strategy can be built up beginning with any initial guess for specifications ¬ J t=0, ht=0 by eqn (15)

$$h_i^{t+1}(a) \leftarrow h_i^t(a) + \eta_h \frac{\partial \mathcal{L}(\{s^\mu || \mathbf{J}^t, \mathbf{h}^t)}{\partial h_i(a)}$$

$$J_{ij}^{t+1}(a,b) \leftarrow J_{ij}^t(a,b) + \eta_j \frac{\partial \mathcal{L}(\{\boldsymbol{s}^\mu\}|\mathbf{J}^t, \mathbf{h}^t)}{\partial J_{ij}(a,b)} \quad (15)$$

until a predetermined point is attained. The learning rates for fields h and coupling parameters J are denoted by ηh and ηJ, respectively. The averages of simple observables across Boltzmann measure Eq. 16 with specifications at iteration time t are included in the gradient terms, as demonstrated by a straightforward calculation:

$$\frac{\partial \mathcal{L}(\{\mathbf{s}^\mu || \mathbf{J}^t, \mathbf{h}^t)}{\partial h_i(a)} = f_i(a) - p_i^{(t)}(a)$$

$$\frac{\partial \mathcal{L}(\{\boldsymbol{s}^\mu\}|\mathbf{J}^t, \mathbf{h}^t)}{\partial J_{ij}(a,b)} = f_{ij}(a,b) - p_{ij}^{(t)}(a,b) \quad (16)$$

When left-hand sides of equations equal zero, that is, when empirical frequency counts for the single and double residues match one- and two-site marginals pi(a) and pij(b) of method P, stationary point is attained. The next sections will provide a formal definition of these quantities. Unable to precisely calculate the marginal probability distributions despite method very straightforward form. In order to address unobserved symbol pairings in one or two columns of the MSA, we supplement the empirical frequency counts by a tiny pseudo-count α. This stops the formation of parameters linked to vanishing empirical frequencies that are infinitely huge (in absolute value). Lastly, the frequencies for one and two sites are provided by eqn (17)

$$f_i(a) = (1-\alpha) f_i^{\text{data}}(a) + \frac{\alpha}{q},$$

$$f_{ij}(a,b) = (1-\alpha) f_{ij}^{\text{data}}(a,b) + \frac{\alpha}{q^2} \quad (17)$$

where f_i^{data} and f_{ij}^{data} are computed from the MSA as eqn (18)

$$f_i^{\text{data}}(a) = \frac{1}{M_{\text{eff}}} \sum_\mu \; w^{\mu i} \delta_{i_\mu^\mu},$$
$$f_{ij}^{\text{data}}(a,b) = \frac{1}{M_{\text{eff}}} \sum_\mu \; w^\mu \delta_{\delta_i^\mu} \delta_{\delta_{j,b},} \qquad (18)$$

with $M_{\text{eff}} = \sum_\mu w^\mu$ being effective number of weighted sequences.

The gradient is then made up of two terms: the first one takes into consideration the interaction between the training set and the RBM's response, while the second one uses the machine-drawn samples. The LL gradient's expression with respect to all the parameters is provided by eqn (19)

$$\frac{\partial \mathcal{L}}{\partial w_{ia}} = \langle v_i h_a \rangle_{\mathcal{D}} - \langle v_i h_a \rangle_{\mathcal{H}}, \; \frac{\partial \mathcal{L}}{\partial b_i} = \langle v_i \rangle_{\mathcal{D}} - \langle v_i \rangle_{\mathcal{H}} \text{ and } \frac{\partial \mathcal{L}}{\partial c_a} = \langle h_a \rangle_{\mathcal{D}} - \langle h_a \rangle_{\mathcal{H}} \qquad (19)$$

where the average over the dataset is indicated by hf(v, h)iD = M−1 P m P {h} f(v (m), h)p(h|v (m)), and the average over the Boltzmann measure is indicated by hf(v, h)iH in Eq. 2.

6. Experimental analysis

Experiments are carried out using Colab on Core-I3 systems with 13GB of RAM from Google Colab Laboratory and 8GB on the PC. For testing, the 4 CPU's 1.7 GHz processor is used. The data set is divided into three parts: the detection set, the cross-validation set, testing set. K-Fold Cross-validation was used. 70% of dataset is utilized as a detection set; remaining 30% is utilized for testing. Cross validation is used for both the testing and detection sets.

Dataset:

Bern Dataset: Image pixel size: 301 × 301 Source of data: ERS-2 satellite SAR sensor Dates of filming: April and May 1999 Scenario: The River Aare flooded the whole city of Thun and Bern, including the Bern airport. Open Source: Github's Yolalala/RS-source

San Francisco Dataset: The image's pixel size is 256 x 256. Data source: ERS-2 satellite SAR sensor, shot between August 2003 and May 2004. Situation: At coordinates 37°28'N, 121°58'W, a populated region stretches across the American city of San Francisco. Open Source: Github's Yolalala/RS-source

Farmland Dataset: The image's pixel size is 257 x 289. The data sensor is the SAR sensor on the Radarsat-2 satellite. Shooting took place on June 18, 2008, and June 19, 2009. Situation: Because of newly planted areas close to the Yellow River Estuary in China. The equivalent image kinds are single-look and four-look multi-temporal images, which are affected by noises of different intensities.

Table 1: Comparative analysis for BERN dataset

Technique	Random accuracy	Average precision	Sensitivity	Specificity
CNN	70	75	76	79
LSTM	79	81	82	80
WKMTNN_DQRBM	89	87	86	90

Table 2: Comparative analysis for SAN FRANCISCO dataset

Technique	Random accuracy	Average precision	Sensitivity	Specificity
CNN	68	72	75	73
LSTM	75	78	81	77
WKMTNN_DQRBM	90	83	88	89

Table 3: Comparative analysis for FARMLAND dataset

Technique	Random accuracy	Average precision	Sensitivity	Specificity
CNN	82	75	80	78
LSTM	88	83	85	84
WKMTNN_DQRBM	98	96	93	95

The above table-1-3 shows Comparative analysis based on various smart grid security dataset. Dataset analysed are MIMIC-IV, SAN FRANCISCO, FARMLAND dataset in terms of Random accuracy, average precision, sensitivity, Specificity.

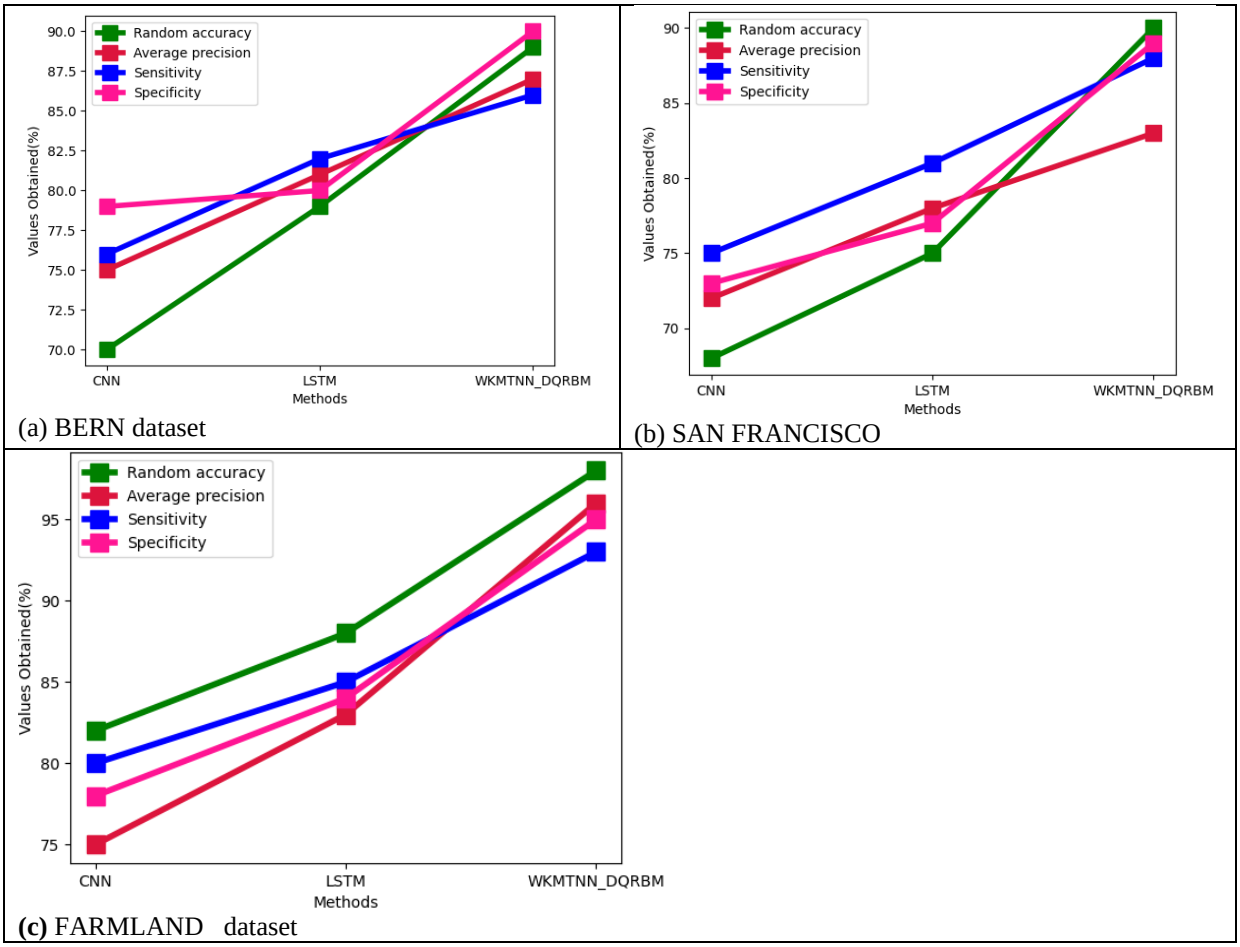

Figure 2. (a)- (c) parametric analysis of existing CNN for (a) MIMIC-IV, (b) SAN FRANCISCO **, (c)** FARMLAND dataset

Figure-2 (a) - (c) shows parametric analysis of existing CNN in BERN dataset. For BERN dataset existing CNN average precision 75%, sensitivity 76%, random accuracy 70%, Specificity 79%. average precision 72%, sensitivity 75%, random accuracy 68%, Specificity 73% for SAN FRANCISCO; CNN average precision 75%, sensitivity 80%, random accuracy 82%, Specificity 78% for FARMLAND dataset.

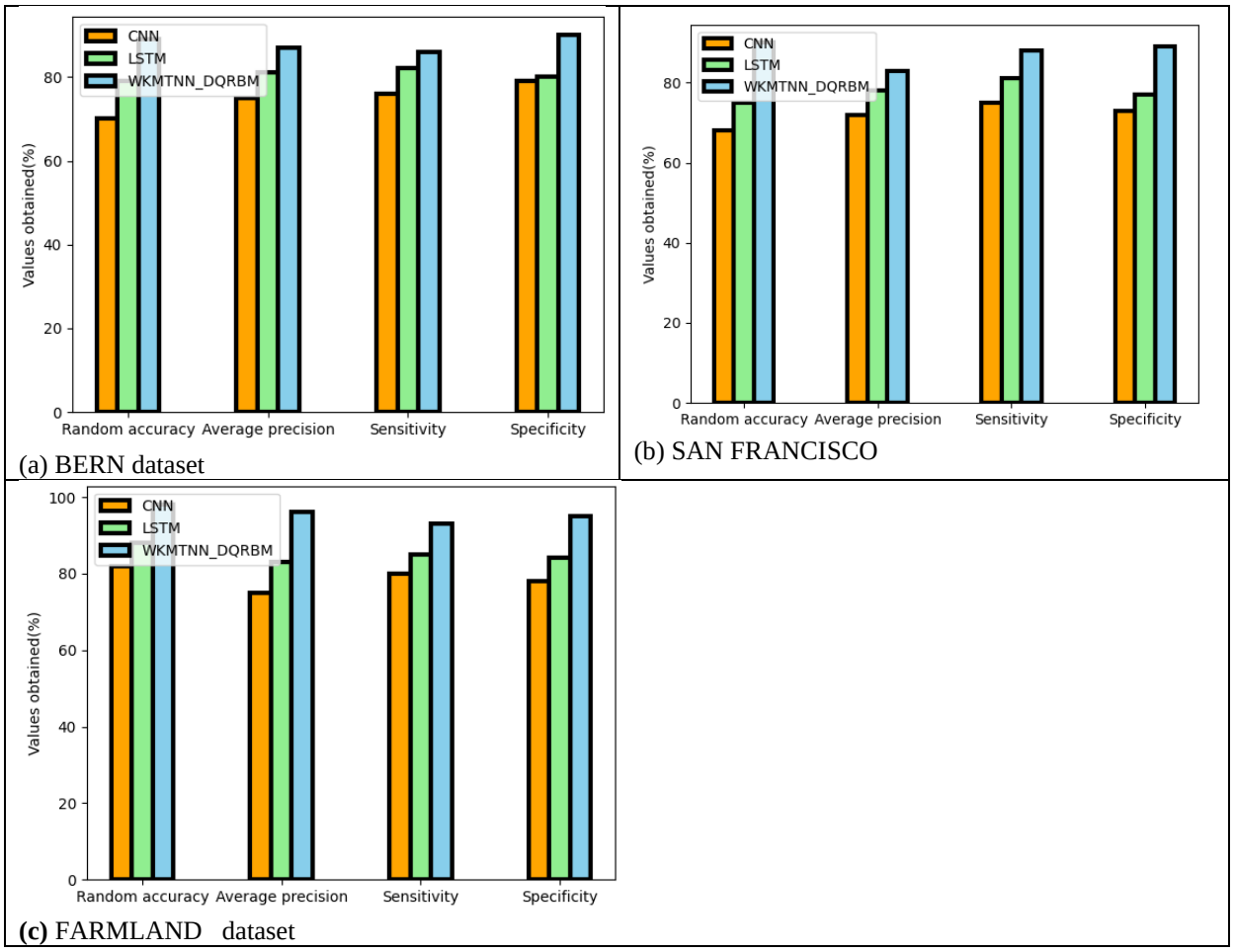

Figure 3. (a) - (c) parametric analysis of existing LSTM for (a) MIMIC-IV, (b) SAN FRANCISCO , (c) FARMLAND dataset

Figure 3(a)–(c) above displays a parametric analysis of LSTM in BERN dataset. LSTM average precision 81%, sensitivity 82%, random accuracy 79%, Specificity 80% on BERN dataset. For SAN FRANCISCO, existing LSTM achieved average precision 78%, sensitivity 81%, random accuracy 75%, Specificity 77%; average precision 83%, sensitivity 85%, random accuracy 88%, Specificity 84% for FARMLAND dataset.

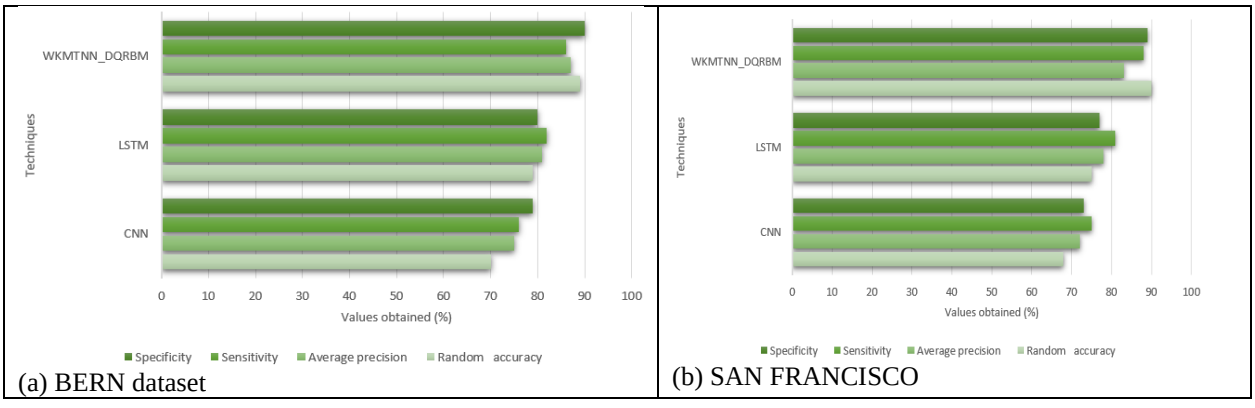

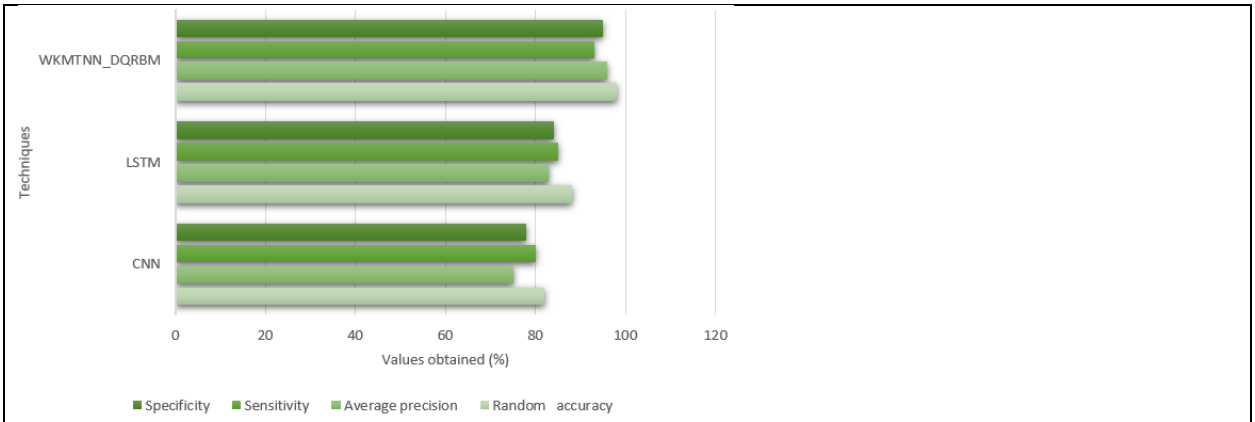

(c) FARMLAND dataset

Figure 4. (a) - (c) parametric analysis of WKMTNN_DQRBM for (a) MIMIC-IV, (b) SAN FRANCISCO **, (c)** FARMLAND dataset

Parametric analysis of WKMTNN_DQRBM in BERN dataset is displayed in above figure 4(a)–(c). WKMTNN_DQRBM achieved 87% average precision, 86% sensitivity, 89% random accuracy, 90% Specificity for BERN dataset. For SAN FRANCISCO, average precision 83%, sensitivity 88%, random accuracy 90%, Specificity 89%. For FARMLAND dataset, average precision 96%, sensitivity 93%, random accuracy 98%, and Specificity 95%.

F=1, N=2, NI=1, and we varied T from 35 to 70. Since there are seven samples each day, it implies the need to employ input series consisting of two values in predicting the plant sickness in a range of five to ten days. Because they were not always available, we only integrated one image instead. We possess a couple of them which vary from 1,930 (T=35) to 1,790 (T=70) based on the value of the parameter T. We have carried out some modifications to the architecture represented in figure 3 because of the few samples. The sensors part is composed of six input series of two elements each. Method is built utilizing Keras framework. We also opted to use Adam as the optimizer with decay 0.0005 and learning rate 0.001. Training and test sets are composed respectively of 80% and 20% of examples. First, feature selection could potentially eliminate extraneous or noisy data that could bewilder the model by decreasing the quantity of features and samples. Second, GRU's ability to identify underlying patterns is improved by focusing on the most pertinent data. Third, with fewer features, GRU is less likely to overfit the training set. In other words, GRU is less likely to suffer from the curse of dimensionality. The curse of dimensionality occurs when a model becomes overly specialized to the training data and underperforms on new data, which can affect complex models with many attributes. Since they can do significantly more work than traditional methods, agricultural drones have completely changed how farmers map, monitor, and spray their crops. Farmers to capture in-depth aerial photos of their farms use drones equipped with sophisticated sensors, cameras, and GIS systems. The information gathered can be utilized to track growth patterns, identify weeds, and pinpoint areas of agricultural stress. Farmers can better control weeds and apply pesticides with the use of this knowledge. Agricultural drones provide high-definition photos that help farmers make decisions about crop growth and maintenance. Additionally, drone-based farming is quicker and more accurate. In fields where their full potential may be realized, like applying pesticides and fertilizers to crops, drones are perfect for precision movement. As a result, there is less waste and environmental harm. Drones also save time and money by automating laborious and time-consuming tasks that would otherwise be done by hand.

As for the benchmarks, the performance metrics have improved significantly. However, angle attention model performs much better than band attention model. Considering that remote sensing images cover a large field of view, this paper claims that the angle information in such images enhances the cloud detection accuracy much more than the band information. This is because data taken from different perspectives contains a cloud boundary shift due to the different angles of view. In order to improve the cloud recognition performance, the angle based channel attention method will focus on learning the degree of channels that are slightly off the true value. Additionally, we can see that the angle attention is near to our performance and the band attention has the biggest gap when compared to the network we proposed. This suggests that in this task, angle information is more useful than band information. Angle attention outcomes are weakened by the concatenation fusion technique. In order to get information that is more useful from the band and angle in upcoming trials, we decided to use the maximum fusion strategy.

7. Conclusion

This research study seeks to devise an innovative approach for the assessment of the sustainability of agriculture in practice by incorporating cloud-based IoT models, deep learning and remote sensing applications. Thus, in this study, field-based analysis of agricultural applications of remote sensing incorporates the cloud IoT model. Watershed K-means temporal neural network (WKMTNN) served to segment this image and deep quantile regressive Boltzmann machine (DQRBM) was used for its classification. The accuracy of detection using this dataset indicated that proposed network has been applied on similar types of remote sensing picture data from various satellite systems. Although this experimental result affirms the effectiveness of our approach, it however is hampered by the available data we have and therefore the need for data augmentation. In the follow-up studies, we will try to tackle issues of limited data sets as well as complex manual data annotation using unsupervised or semi-supervised learning.

References

[1] A. Morchid, M. Marhoun, R. El Alami, and B. Boukili, "Intelligent detection for sustainable agriculture: A review of IoT-based embedded systems, cloud platforms, DL, and ML for plant disease detection," *Multimedia Tools Appl.*, pp. 1–40, 2024.

[2] M. Peng *et al.*, "Crop monitoring using remote sensing land use and land change data: Comparative analysis of deep learning methods using pre-trained CNN models," *Big Data Res.*, vol. 36, p. 100448, 2024.

[3] P. Chinnasamy *et al.*, "Crop Optimization and Disease Detection using Satellite Imagery & Artificial Intelligence," in *Proc. Second Int. Conf. Intell. Cyber Phys. Syst. Internet Things (ICoICI)*, Coimbatore, India, 2024, pp. 1531–1535.

[4] Y. N. Altherwy, A. Roman, S. R. Naqvi, A. Alsuhaibani, and T. Akram, "Remote Sensing Insights: Leveraging Advanced Machine Learning Models and Optimization for Enhanced Accuracy in Precision Agriculture," *IEEE Access*, 2024.

[5] Y. B. Kalpana *et al.*, "Revolutionizing Agriculture: Integrating IoT Cloud, and Machine Learning for Smart Farm Monitoring and Precision Agriculture," in *Computational Intelligence in Internet of Agricultural Things*, Cham: Springer, 2024, pp. 79–108.

[6] P. Chinnasamy, R. Geetha, S. Geetha, S. P. Balakannan, K. Ramprathap, and V. Praveena, "Secure Smart Green House Farming using Blockchain Technology," *Turk. J. Comput. Math. Educ.*, vol. 12, no. 6, pp. 2858–2865, 2021.

[7] A. Mulakaledu *et al.*, "Satellite Image–Based Ecosystem Monitoring with Sustainable Agriculture Analysis Using Machine Learning Model," *Remote Sens. Earth Syst. Sci.*, pp. 1–10, 2024.

[8] G. B. C. Narayanappa *et al.*, "Revolutionizing UAV: Experimental Evaluation of IoT-Enabled Unmanned Aerial Vehicle-Based Agricultural Field Monitoring Using Remote Sensing Strategy," *Remote Sens. Earth Syst. Sci.*, pp. 1–15, 2024.

[9] R. Manoharan, "Improving Security and Performance in Chaotic Optical Communication via Real-Time Pilot Signal Processing Techniques," *IETE J. Res.*, pp. 1–9, 2025.

[10] M. Rajesh, S. Ramachandran, K. Vengatesan, S. S. Dhanabalan, and S. K. Nataraj, "Federated Learning for Personalized Recommendation in Securing Power Traces in Smart Grid Systems," *IEEE Trans. Consum. Electron.*, vol. 70, no. 1, pp. 88–95, Feb. 2024.

[11] V. C. S. S, A. Hareendran, and G. F. Albaaji, "Precision farming for sustainability: An agricultural intelligence model," *Comput. Electron. Agric.*, vol. 226, p. 109386, 2024.

[12] M. M. Metwaly, M. A. AbdelRahman, and S. A. Mohamed, "A Machine Learning Model and Multi-Temporal Remote Sensing for Sustainable Soil Management in Egypt's Western Nile Delta," *Earth Syst. Environ.*, pp. 1–21, 2024.

[13] E. A. Al-Shahari *et al.*, "Internet of Things Assisted Plant Disease Detection and Crop Management using Deep Learning for Sustainable Agriculture," *IEEE Access*, 2024.

[14] H. M. Albarakati *et al.*, "A Novel Deep Learning Architecture for Agriculture Land Cover and Land Use Classification from Remote Sensing Images Based on Network-Level Fusion of Self-Attention Architecture," *IEEE J. Sel. Topics Appl. Earth Observ. Remote Sens.*, 2024.

[15] E. Asmar, M. H. Vahidnia, M. Rezaei, and E. Amiri, "Remote sensing-based paddy yield estimation using physical and FCNN deep learning models in Gilan province, Iran," *Remote Sens. Appl.: Soc. Environ.*, vol. 34, p. 101199, 2024.

[16] E. López-Pérez, C. Sanchis-Ibor, M. Á. Jiménez-Bello, and M. Pulido-Velazquez, "Mapping of irrigated vineyard areas through the use of machine learning techniques and remote sensing," *Agric. Water Manage.*, vol. 302, p. 108988, 2024.

[17] Chatrabhuj and K. Meshram, "Incremental learning model for sustainable agricultural land assessment using multimodal satellite data," *Int. J. Remote Sens.*, pp. 1–27, 2024.

[18] C. Trentin, Y. Ampatzidis, C. Lacerda, and L. Shiratsuchi, "Tree crop yield estimation and prediction using remote sensing and machine learning: A systematic review," *Smart Agric. Technol.*, p. 100556, 2024.

[19] A. A. Pinto, C. Zerbato, and G. de Souza Rolim, "A machine learning models approach and remote sensing to forecast yield in corn with based cumulative growth degree days," *Theor. Appl. Climatol.*, vol. 155, no. 8, pp. 7285–7294, 2024.